RSC Advances

PAPER

View Article Online
View Journal | View Issue

Cite this: *RSC Adv.*, 2019, **9**, 14443

A practical non-enzymatic urea sensor based on $NiCo_2O_4$ nanoneedles†

Sidra Amin,[abc] Aneela Tahira,[a] Amber Solangi,[b] Valerio Beni,[e] J. R. Morante,[d] Xianjie Liu,[f] Mats Falhman,[f] Raffaello Mazzaro,[a] Zafar Hussain Ibupoto *[ag] and Alberto Vomiero *[a]

We propose a new facile electrochemical sensing platform for determination of urea, based on a glassy carbon electrode (GCE) modified with nickel cobalt oxide ($NiCo_2O_4$) nanoneedles. These nanoneedles are used for the first time for highly sensitive determination of urea with the lowest detection limit (1 μM) ever reported for the non-enzymatic approach. The nanoneedles were grown through a simple and low-temperature aqueous chemical method. We characterized the structural and morphological properties of the $NiCo_2O_4$ nanoneedles by TEM, SEM, XPS and XRD. The bimetallic nickel cobalt oxide exhibits nanoneedle morphology, which results from the self-assembly of nanoparticles. The $NiCo_2O_4$ nanoneedles are exclusively composed of Ni, Co, and O and exhibit a cubic crystalline phase. Cyclic voltammetry was used to study the enhanced electrochemical properties of a $NiCo_2O_4$ nanoneedle-modified GCE by overcoming the typical poor conductivity of bare NiO and Co_3O_4. The GCE-modified electrode is highly sensitive towards urea, with a linear response ($R^2 = 0.99$) over the concentration range 0.01–5 mM and with a detection limit of 1.0 μM. The proposed non-enzymatic urea sensor is highly selective even in the presence of common interferents such as glucose, uric acid, and ascorbic acid. This new urea sensor has good viability for urea analysis in urine samples and can represent a significant advancement in the field, owing to the simple and cost-effective fabrication of electrodes, which can be used as a promising analytical tool for urea estimation.

Received 2nd February 2019
Accepted 14th April 2019

DOI: 10.1039/c9ra00909d

rsc.li/rsc-advances

Introduction

Urea (also known as carbamide, carbonyl diamide) is a biomolecule and the major final metabolite of nitrogenous compounds in living organisms, accounting for 70–80% of nitrogen excretion in humans. Urea is present in urine or blood and is deeply investigated in clinical studies. It is extensively used as fertilizer and present in a variety of food products. Therefore its selective and sensitive monitoring through cost effective methodologies is very important.[1] In the human body, urea is formed exclusively in the liver, and it is transported by the bloodstream to the kidneys, where it is excreted into the urine,[2] as an end product of protein metabolism.[3] Several methods have been developed for the detection of small biomolecules using nanostructure materials[4–6]

To date several analytical methods have been proposed for the determination of urea, such as high performance liquid chromatography (HPLC),[7,8] gas chromatography (GC)[9],[14]N-NMR,[10] infrared (IR) spectrometry,[11,12] calorimetry,[13] fluorimetry,[14] and chemiluminescence.[15] All these methods for the determination of urea are either costly or require expertise in handling the instruments and are not suitable for field measurements.[16,17] Another strategy for urea determination is through electrochemical sensing/biosensing, by potentiometric measurements in the configuration of ion selective electrode and ammonium ion-generating enzyme,[18] where poly(vinyl alcohol) containing styrylpyridinium PVA/SbQ membrane[19] are commonly employed. However, potentiometric urea biosensors have intrinsic limitations such as high interference with competing species such as uric acid, Na^+, K^+ ions, *etc.*, high detection limit and slow response time (see Table 1). Additionally, urea biosensors based on copolymer indium-tin-oxide

[a]*Division of Materials Science, Department of Engineering & Mathematics, Luleå University of Technology, 97187 Luleå, Sweden. E-mail: Alberto.vomiero@ltu.se; zafar.ibupoto@ltu.se*

[b]*National Centre of Excellence in Analytical Chemistry, University of Sindh, Jamshoro 76080, Pakistan*

[c]*Department of Chemistry, Shaheed Benazir Bhutto University, Shaheed Benazirabad 67450, Sindh, Pakistan*

[d]*Catalonia Institute for Energy Research (IREC), Jardins de les Dones de Negre 1, Sant Adrià del Besòs, Barcelona 08930, Catalonia, Spain*

[e]*RISE Acreo, Research Institute of Sweden, Norrköping, Sweden*

[f]*Department of Physics, Chemistry and Biology, Surface Physics and Chemistry, Linköping University, Faculty of Science & Engineering, Sweden*

[g]*Institute of Chemistry, University of Sindh, Jamshoro 76080, Sindh, Pakistan*

† Electronic supplementary information (ESI) available. See DOI: 10.1039/c9ra00909d

Table 1 Analytical application of $NiCo_2O_4$ nanoneedle-modified/GCE urea sensor for the quantification of urea from diluted urine samples

Sample	Added (mM)	Detected (mM)	Recovery (%)
1	0	0.28 ± 0.03	
	0.5	0.50 ± 0.03	100.7
	1	0.95 ± 0.04	95.2
	1.5	1.52 ± 0.21	101.6
2	0	0.28 ± 0.01	
	0.5	0.52 ± 0.05	104.8
	1	0.96 ± 0.03	96.3
	1.5	1.45 ± 0.36	97.1
3	0	0.15 ± 0.48	
	0.5	0.49 ± 0.22	99.2
	1	1.04 ± 0.04	104.7
	1.5	1.52 ± 0.59	101.7

(ITO),[3] CH–Fe_3O_4/TiO_2,[20] electrochemical hydrolase-based and creatinine biosensors[21] involve complicated steps in the fabrication of electrode, which are not economically feasible and environmental friendly.

Therefore, it is desired to develop a user-friendly method for direct in field urea measurement. Suitably designed nanomaterials can offer specific functionalities for the purpose. The catalytic, electrochemical and electric properties of nanostructured oxide materials strongly depend on their size, shape and surface morphology.[22–26] Specifically, the electronic and surface properties of 1- and 2-dimensional nanostructures, such as large specific surface area, mechanical stability, low potential either for oxidation or reduction, light weight, fast electron transport are useful for the development of advanced electrochemical biosensors and sensors.[27,28] Non-enzymatic biosensors with metal-based catalysts have been widely used due to their high stability and enhanced sensitivity. Transition metal oxides such as CuO, ZnO, and NiO have been widely used for the determination of urea.[29] However, these nanostructures used urease enzyme and exhibit poor performance, not allowing their practical applications. In particular, the drawback of NiO nanostructures used in the non-enzymatic urea senor is its poor conductivity, limiting the response to a narrow range of urea concentration and high detection limit.[30] The bottleneck in CuO 1-D sensors is that it is a very challenging task to get abundant CuO nanowires by low temperature aqueous chemical growth methods, thus limiting the possibility of scaling up. ZnO nanostructures exhibit poor catalytic properties that limits its wide spread applications in non-enzymatic technology for the detection of various analytes. For these reasons, the investigation of a new class of sensors is highly welcome. The use of bimetallic oxide nanostructure can help by mitigating the issue of poor electrical conductivity and slow charge transfer processes. They demonstrated of great interest for the development of future devices, like, for instance, in supercapacitors due to their fast charge transfer kinetics. Among them, nickel cobalt oxide ($NiCo_2O_4$) exhibits electron conductivity two orders of magnitude larger than pure NiO or Co_3O_4. Therefore, it has been used in diverse applications.[31–33] However, there is no report on non-enzymatic urea sensor based on 1-D metal oxides, which deserve to be investigated owing to their outstanding physical and electronic properties of these nanostructures.

In the present work, we demonstrated for the first time the electrochemical determination of urea by using $NiCo_2O_4$ nanoneedle-modified glassy carbon electrode (GCE). Electroanalytical detection based on the use of nanoneedle-modified GCE for urea sensing can offer a practically viable method, free from sample pretreatment, long analysis time and sophisticated experimental setup. The modified electrode was also used for the quantification of urea from real samples.

These results offer a new opportunity towards the development of non-enzymatic urea sensors for clinical analyses and hospitals, in which highly sensitivities and broad range of linear response for urea detection are required. Further development includes the tuning of the nanostructure morphology or the use of three-dimensional porous supporting material for the growth of 1-D hierarchical nanostructures.

Experimental

The scheme of production of the new electrode and its application as urea sensor is illustrated in Fig. 1, from the synthesis of the oxide nanomaterials, to the test as non-enzymatic urea sensor.

Reagents and solutions

Cobalt chloride hexahydrate ($CoCl_2 \cdot 6H_2O$), nickel chloride hexahydrate ($NiCl_2 \cdot 6H_2O$), urea (CH_4N_2O), were purchased from Sigma-Aldrich (Stockholm, Sweden) and used without any further purification. All chemicals were of analytical grade reagents and were used as received.

All glassware was washed by soaking in 3 M HNO_3 overnight followed by washing with detergent water. It was then thoroughly washed with tap water and finally rinsed at least 3 times with doubly distilled water. The glassware was then dried in an oven at 110 °C.

Synthesis of $NiCo_2O_4$ nanoneedles and fabrication on glassy carbon electrode

Aqueous chemical growth method at low temperature has been applied for the development of $NiCo_2O_4$ nanostructures. For this purpose, 2.37 g of cobalt chloride hexahydrate, 1.185 g of nickel chloride hexahydrate and 2 g of urea were dissolved in 75 mL of Milli-Q water and stirred for 30 min, and then the beaker containing the growth solution was covered completely with aluminum foil and kept in a preheated oven at 95 °C for 5 h. After that $NiCo_2O_4$ nanostructures were taken out by filtration from the growth solution and washed with Milli-Q water. In last step at room temperature sample were dried and additionally these nanostructures were annealed at 500 °C for 3 h to convert nickel cobalt hydroxide into nickel cobalt oxide phase.

10 mg of $NiCo_2O_4$ nanoneedles were prepared in 2.5 mL of Milli-Q water and sonicated for 15 min, after that 500 μL of Nafion (5%) was added in it, based on previous investigations.[34] Then the GCE was polished with alumina powder, covered with

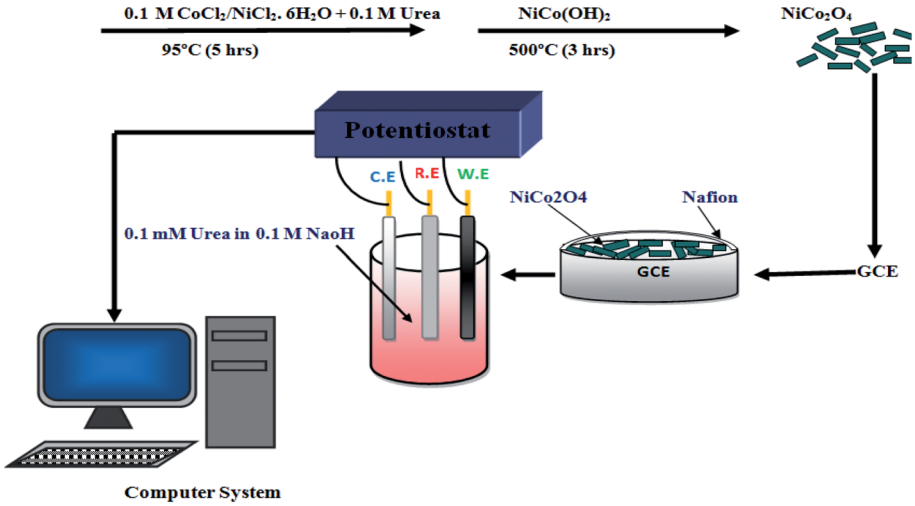

Fig. 1 Scheme for the fabrication of the non-enzymatic urea sensor based on $NiCo_2O_4$ nanoneedle-modified GCE, from nanomaterials synthesis, to sensor testing.

5 μL of $NiCo_2O_4$ nanoneedles with weight of 0.2 mg by drop casting, dried for 10 min at room temperature, and then ready to be used for urea measurements. The presence of Nafion guarantees the good adhesion of the nanoneedles to the GCE.

Synthesis of NiO and Co_3O_4 benchmarking electrodes

NiO nanostructures were synthesized by low temperature aqueous chemical growth method using a two-step approach. First, nickel hydroxide was obtained by mixing equi-molar 0.1 M concentration of nickel chloride hexahydrate and hexamethylenetetramine in a glass beaker of 100 mL capacity. The growth solution was covered with aluminum foil and kept in preheated electric oven at 95 °C for 5 hours. After the completion of the growth, the nickel hydroxide nanostructured material was obtained by filtration and washed several times with deionized water and ethanol. Then nickel hydroxide nanostructures were calcinated at 450 °C for 3 hours in air and NiO nanostructured material was successfully obtained. Likewise, nanostructured Co_3O_4 was prepared by the same two-step procedure, by using different precursors, *i.e.* 0.1 M $CoCl_2 \cdot 6H_2O$ and urea, under the same experimental conditions described above.

Morphology and structure

The shape evolution of $NiCo_2O_4$ nanostructures was investigated by high resolution LEO 1550 Gemini field emission scanning electron microscope working at 10 kV. The crystal quality was evaluated by X-ray powder diffraction (XRD) of Phillips PW 1729 powder diffractometer using CuKα radiation ($\lambda = 1.5418$ Å), a generator voltage of 40 kV and a current of 45 mA.

HRTEM and STEM images have been obtained by using a FEI Tecnai F20 field emission gun microscope with a 0.19 nm point-to-point resolution at 200 kV equipped with an embedded Quantum Gatan Image Filter for EELS analyses. Images have been analyzed by means of Gatan kDigital Micrograph software. The X-ray photoelectron spectroscopy (XPS) experiments were carried out using a Scienta ESCA 200 spectrometer in ultrahigh vacuum at a base pressure of 10^{-10} mbar with a monochromatic Al (K alpha) X-ray source providing photons with 1486.6 eV. The XPS experimental condition was set so that the full width at half maximum of the clean Au $4f_{7/2}$ line was 0.65 eV. All spectra were collected at a photoelectron takeoff angle of 0° (normal emission) at room temperature.

Functional characterization

All voltammetry measurements were carried out by using a CHI 760D Electrochemical Workstations. The software CHI 9.22 (Austin, USA) was used in combination with the electrochemical workstation. A conventional assembly of three-electrode system was used. The maximum capacity of solution in cell was 5–10 mL with gas bubbler and gas outlet ports.

GCE with a diameter of 2 mm used as working electrodes, in combination with platinum (Pt) wire as counter and Ag/AgCl as reference electrode (purchased from CHI Austin, USA) were used as received. The working electrodes were manually cleaned before each scan by mechanical polishing using alumina powder.

Solution of 0.1 M NaOH (E. Merck-Germany) was prepared in Milli-Q water and was used as supporting electrolyte. A stock solution of 100 mM urea was prepared in sodium hydroxide. The low concentration standard solutions of urea were freshly prepared before the measurements by dilution. Stock solution of Nafion (5%) (Sigma Aldrich) was prepared in isopropanol. All the measurements were performed at room temperature. The peak current in cyclic voltammetry curve for urea oxidation was found around +0.75 V *vs.* Ag/AgCl reference electrode.

Results and discussion

Fig. 2 shows the SEM and ADF-STEM images of $NiCo_2O_4$ nanoneedles. These nanoneedles are formed by the self-assembly of nanoparticles. The EELS chemical composition

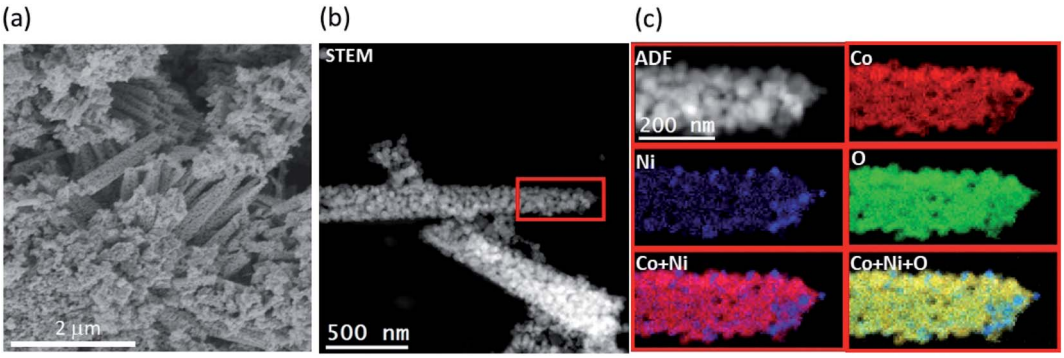

Fig. 2 (a) SEM and (b) ADF STEM images of $NiCo_2O_4$ nanoneedles. (c) EELS elemental distribution maps obtained with the Co $L_{2,3}$-edge (red), Ni $L_{2,3}$-edge (blue), O K-edge (green) and their color composite in $NiCo_2O_4$ nanoneedles from the red squared area in (b).

maps for Co, Ni and O obtained from the ADF-STEM micrograph are also reported. The compositional analysis (also confirmed in Fig. S1†) indicates that the nanoneedles are composed of evenly distributed Co, Ni and O, as expected. Fig. 3 (left panel) shows the TEM microscopy on a single particle, including its high resolution and FFT analysis. The FFT spectrum indicates that the material crystallizes in the cubic Co_3O_4/$NiCo_2O_4$ phase, [kFD3-MZ]-space group 227, with lattice parameters $a = b = c = 0.8065/0.8114$ nm, and $\alpha = \beta = \gamma = 90^\circ$ as visualized along the [0–11] direction. Further HRTEM analysis revealed also the presence of cubic phase of NiO, as shown in Fig. S2.† The morphology and structure of the NiO and Co_3O_4 nanostructures are reported in Fig. S3–S7.† NiO presents a flower sheet-like structure (Fig. S3 and S4†) with a cubic crystalline phase (Fig. S5†). The Co_3O_4 presents a nanowire-like structure, as visible in Fig. S6,† with a diffraction pattern ascribable to a cubic structure (Fig. S7†).

The EDS analysis (Fig. S8(a–c)†) indicated the expected composition for (a) NiO and (b) Co_3O_4, and (c) the presence of ~20.5% in weight of Ni in the composite system, suggesting that, most probably, Ni is incorporated into the $NiCo_2O_4$ phase. The powder X-ray diffraction pattern (Fig. 3 (right panel)) confirmed the presence of reflections from the cubic Co_3O_4 phase (JCPDS card no. = 42-1467) and cubic NiO phase (JCPDS card no. = 04-0835) in samples Co_3O_4 and NiO, respectively, as expected. Reflections from the cubic Co_3O_4 or $NiCo_2O_4$ phase are present in the composite system ($NiCo_2O_4$ – JCPDS card no. = 20-078 and Co_3O_4 cannot be discriminated through XRD),

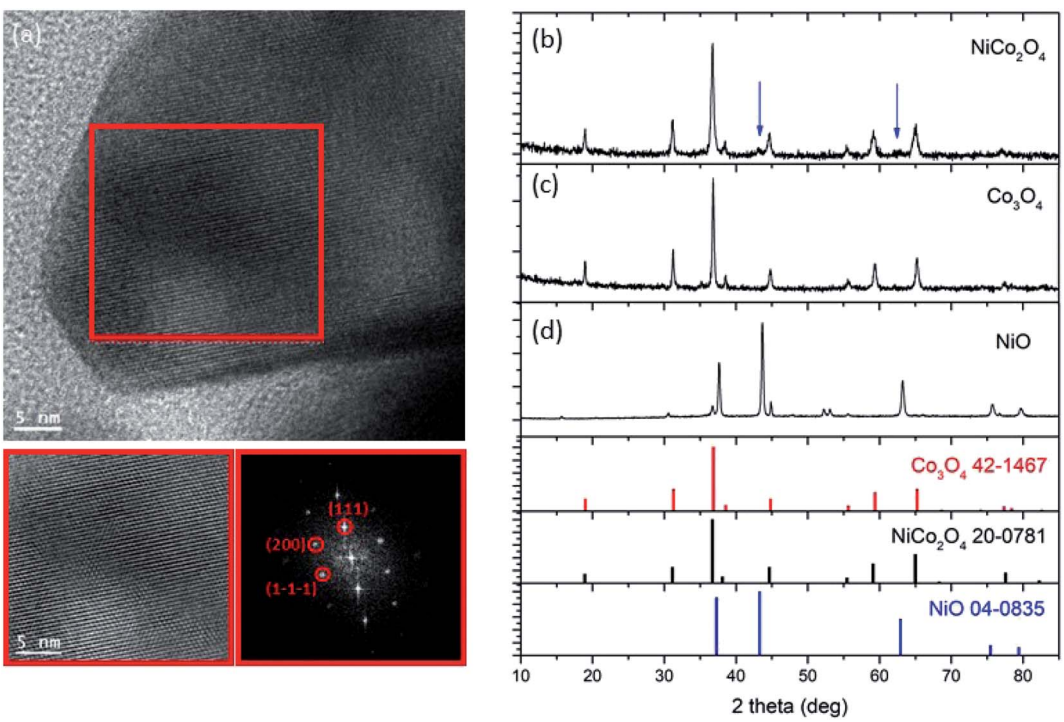

Fig. 3 (Left) High resolution transmission electron microscopy of $NiCo_2O_4$ nanoneedles and FFT spectrum. (Right) Powder XRD spectrum of $NiCo_2O_4$ nanoneedles at room temperature.

together with two low-intensity reflections (blue arrows), which suggest the presence of some NiO phase. From these analyses, we can conclude that the composite system is most likely composed of $NiCo_2O_4$ cubic phase and some residual NiO cubic phase.

The chemical composition of $NiCo_2O_4$ nanomaterial was investigated by X-ray photoelectron microscopy (Fig. 4). The wide scan survey spectrum of the sample confirms the presence of Co, Ni and O. The photoemission peak at binding energy of 780.4 eV corresponds to Co $2p_{3/2}$ and the peak at the binding energy of 796.2 eV corresponds to Co $2p_{1/2}$. Satellite peaks at 786.7 and 802.5 eV binding energy are assigned to Co $2p_{3/2}$ and to Co $2p_{1/2}$, respectively, in agreement with the previous literature. The Ni $2p_{3/2}$ peak at 855.1 eV and Ni $2p_{1/2}$ peak at 873.2 eV are also present, indicating the presence of NiO.[35]

The nanoneedle/GCE electrode was used for urea detection in 0.1 M NaOH solution containing 0.1 M of urea (Fig. 5). We also tested bare GCE without nanoneedles both in pure electrolyte (black curve) and in presence of 0.1 M urea (red curve). In the inset of Fig. 5(a) we report the response curve for the nanoneedle/GCE in 0.1 M NaOH. When $NiCo_2O_4$ nanoneedle/GCE is used, two clear oxidation and reduction peaks were recorded: one anodic peak at around 750 mV and one cathodic peak at around 550 mV. The analysis of the oxidation/reduction peaks ratio and of the peak to peak separation, as a function of the scan rate (Fig. S13 and Table S2†), recorded at different scan rates, seems to indicate that oxidation/reduction or urea follow a semi-reversible process. It is because of the weak urea adsorption prior to oxidation at the proposed $NiCo_2O_4$ nanoneedle. On the other end, a very weak oxidation signal was recorded, at the bare GCE without nanoneedles (Fig. 5(a)). The results confirm the electro catalytic properties of $NiCo_2O_4$ nanoneedle towards urea.

The proposed enzyme free sensing mechanism for the alkaline oxidation of urea is described as follows, after the immediate absorption of OH-ions, both the Ni^{2+} and Co^{2+} are oxidized into Ni^{3+} and Co^{3+}. Then, both the Ni^{2+} and Co^{2+} are oxidized into Ni^{3+} and Co^{3+}. Moreover, the alkaline mechanism is according to the reported work:[36] later the urea is adsorbed on the NiOOH by Ni–O and O–C coordinate linkages and simultaneous direct oxidation of urea is taking place on NiOOH.[37] Furthermore, the NiOOH is reduced to $Ni(OH)_2$ at the time of urea oxidation. The reported work suggests that cobalt ions are also involved in the oxidation of urea which is poor in response towards urea oxidation that is mainly coming from the presence of Co^{4+}/Co^{3+} active sites.[38]

The cyclic voltammograms of the $NiCo_2O_4$ nanoneedles/GCE in 0.1 M urea solution recorded at different scan rates (between 10 and 100 mV s^{-1}) are reported as an inset in Fig. 5(b). The plot of peak current of urea oxidation has a linear dependence upon the square root of scan rate as shown in Fig. 5(b) indicating the diffusion control of the reaction.

To demonstrate the stability of the $NiCo_2O_4$ nanoneedle and the reproducibility of the measurements, we recorded 16 repetitive runs for 0.1 M of urea (Fig. 6(a)). The relative standard deviation (RSD) for the obtained results was 4%. These results confirm the stability, upon use, of the $NiCo_2O_4$ nanoneedles/GCE electrode and the reproducibility of its electro-catalytic performance over urea oxidation. The specificity of the $NiCo_2O_4$ nanoneedle/GCE electrode to urea was tested toward likely interferences including glucose, ascorbic acid, uric acid and their mixtures. Cyclic voltammetry experiments were carried out for 0.1 M of urea in the presence of equi-molar concentration of each interferent and mixtures of them. Fig. 6(b) represents some of the potential interferents response during the sensing of urea. The response of urea at $NiCo_2O_4$

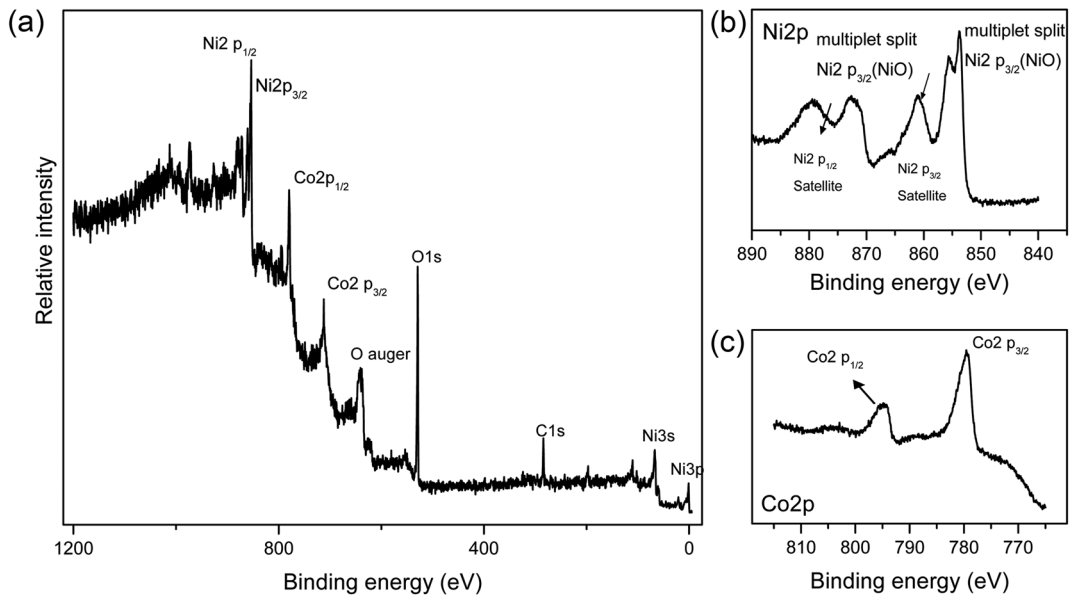

Fig. 4 (a) Wide scan survey XPS spectrum of $NiCo_2O_4$ nanoneedles. (b) Ni 2p spectrum. (c) Co 2p spectrum.

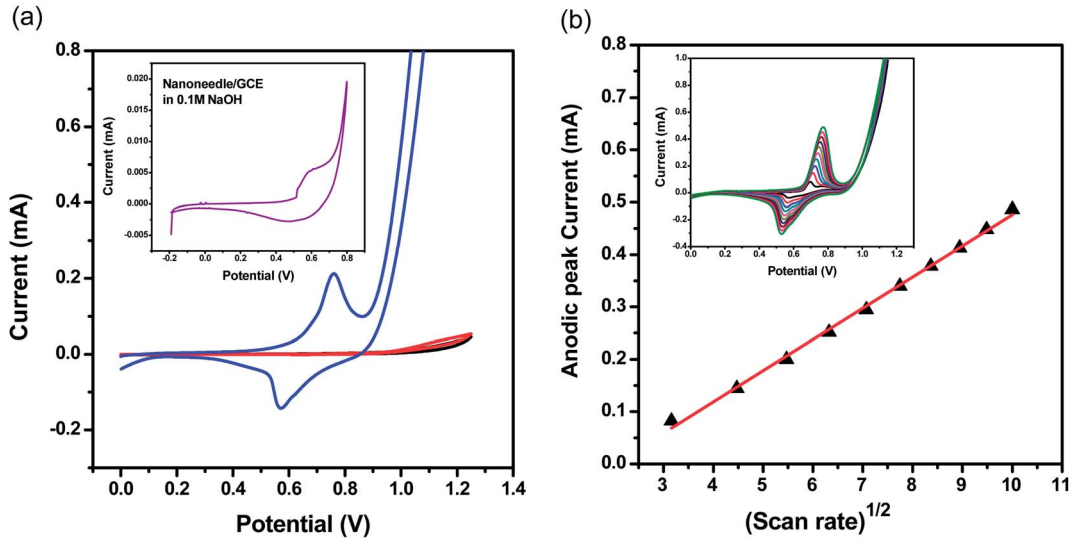

Fig. 5 (a) CV response of bare GCE (red) and $NiCo_2O_4$ nanoneedle/GCE (blue) in 0.1 M urea, and response of bare GCE in blank 0.1 M NaOH (black). Inset: nanoneedle/GCE in 0.1 M NaOH. (b) Anodic peak current of various CV runs *versus* the square root of the scan rate. Inset: CV response of the $NiCo_2O_4$ nanoneedle/GCE electrode in 1 mM urea at different scan rates.

nanoneedle/GCE is not affected by the presence of interferents such as glucose, uric acid and ascorbic acid, demonstrating that the sensor is suitable for selective urea detection in real applications.

The calibration curve at various urea concentrations (Fig. 6(c)) indicates the linear dependence of the recorded current *vs.* different urea concentrations in the range 0.01 to 5 mM inset in (Fig. 6(c)) shows peak current *vs.* urea concentration range from 0.01 to 1 mM. The resulting R^2 value is 0.99, which indicates a good linear behavior of the electrode in the specified concentration range. The corresponding CV runs at different concentrations are enclosed in the ESI (Fig. S9†).

The lower detection limit (LOD) and quantification limit (LOQ) of the proposed sensor were calculated[36] as $DL/DQ = F \times SD/b$, where the factor F is equal to 3.3 and 10 for the detection limit and the limit of quantification, respectively, SD is the standard deviation of the blank, and b is the slope of the linear regression of the calibration curve. The LOD was calculated to be 1.0 μg cm^{-3} and the LOQ was calculated to be 3.6 μg cm^{-1}.[39]

Table S3† collects the comparative data from the literature on various methods and materials used for urea sensing. The overall performance of the $NiCo_2O_4$ nanoneedle/GCE is competitive or even far better than the previously reported sensors. As reported in Table S3,† most of the sensors are urease-based, which makes the system complex and expensive. Additionally, the detection limit of the newly prepared electrode was outstandingly lower than other reported values, representing a significant advancement in the specific field and making the new nanoneedle/GCE electrode a viable candidate for practical use. For the demonstration of the outstanding properties of the $NiCo_2O_4$ nanoneedles, a comparative CV study was performed under the same experimental conditions, applying NiO and Co_3O_4 nanostructures for urea sensing (Fig. S10†). The oxidation peak current in the case of nickel cobalt oxide nanoneedles is highly enhanced compared to both NiO and Co_3O_4, which can be attributed to the excellent electrocatalytic properties of the bimetallic oxides. This is further verified by electrochemical impedance analysis. The Nyquist plot obtained in absence of any faradaic process (+200 mV) was employed for the determination of the double layer capacitance of the electrode materials as shown in Fig. S11,† as described earlier.[40] The C_{DL} values obtained are respectively 0.038 mF cm^{-2} for NiO, 0.044 mF cm^{-2} for Co_3O_4 and 0.059 mF cm^{-2} for $NiCo_2O_4$. The higher C_{DL} value for the bimetallic oxide suggests a larger number of active sites due to the larger electrochemical surface area (assuming comparable specific capacitance). Therefore, we chose to be more conservative and only qualitatively compare the variation of double layer capacitance.[41] The EIS method has been proved to be highly reliable and fully consistent with the CV method, as previously reported.[40]

The developed sensor was successfully applied to the analysis of urine samples. Urine samples were collected from three healthier people (lab mates) after 2 h of their breakfast. Prior to analysis, urine samples were filtered through a 3 μm size of filter paper, to get rid of protein aggregates. The urine samples were diluted in NaOH (supporting electrolyte) at the ratio of 1 : 10 by volume; they were then spiked with known concentrations of urea solutions. The modified electrode was used to analyze three urine samples. The influence of the matrix was examined by performing recovery experiments and the results were estimated from the calibration curve. All experiments were performed three times, to guarantee their reproducibility. Recoveries and % RSD values of each sample are given in Table 1. The CV runs for the determination of urea from real samples are provided in the ESI (Fig. S12†), demonstrating the practical application of the proposed sensor for urea monitoring in real urine samples.

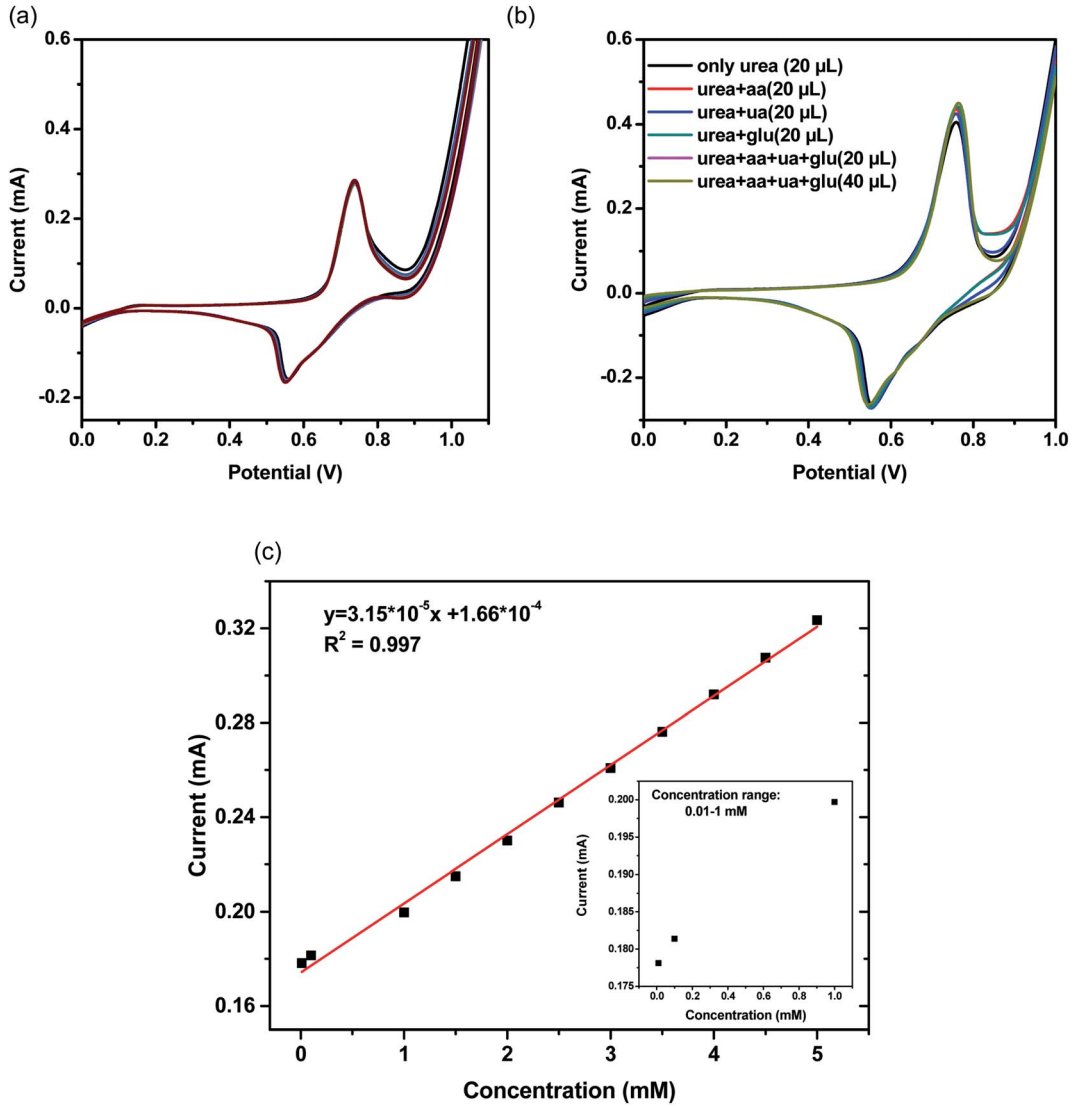

Fig. 6 (a) Sixteen repeated CVs measurements of the $NiCo_2O_4$ nanoneedle-modified/GCE sensor in 0.1 M urea to monitor the stability and reproducibility. (b) Influence of potential interferents on the voltammetry response in 0.1 M urea. (c) Calibration plot (peak current *versus* urea concentration) in the concentration range 0.01–5 mM.

Conclusions

In summary, we proposed bimetallic oxide nanoneedles of $NiCo_2O_4$, synthesized by low temperature aqueous chemical growth method, as new enzyme-free urea sensors. The high purity $NiCo_2O_4$ nanoneedles result from the self-assembly of nanoparticles and exhibit cubic crystalline phase. Owing to their enhanced catalytic activity and conductivity, application of $NiCo_2O_4$ nanoneedles was found highly effective for the selective and sensitive quantification of urea both in chemical sensing and urine samples.

The superior performance of $NiCo_2O_4$ nanoneedle-modified/GCE non-enzymatic urea sensor over urease immobilized electrode matrix biosensors can be used towards the development of non-enzymatic urea sensing. Urease-based biosensors are very selective and sensitive, however they present significant drawbacks, including use of expensive urease enzyme (and need of specific conditions for storage), thermal stability, sensitivity to harsh acidic and alkaline media,[42] and loss of enzyme activity with time[39] The proposed $NiCo_2O_4$ nanoneedle-modified/GCE non-enzymatic urea sensor is highly selective, sensitive and stable, compared to the urease based biosensors, exhibiting the lowest detection limit ever reported, equal to 1.0 μM. The presented protocol for urea measurement has a series of merits compared to the reported literature such as easy accessibility in harsh conditions, including high pH, wide linear range of urea, high reproducibility, facile fabrication process, and does not require specific storage conditions. The $NiCo_2O_4$ nanoneedles are obtained from earth abundant and cheap sources, making them economically viable in both developed and developing countries. The presented urea sensor is enzyme-free, making it a unique configuration, suitable for large scale applications.

We also demonstrated the successfully use of the sensor for the monitoring of urea from urine samples. Our results indicate that the $NiCo_2O_4$ nanoneedle-based urea sensor can be capitalized for routine analysis of urea from various clinical and food samples and represents a significant advancement in the field.

Ethical statement

Experiments related to urine analysis were approved by the ethics committee at Sindh University Jamshoro, Sindh Pakistan. Informed consents were obtained from human participants of this study.

Conflicts of interest

Authors declare no conflict of interest in this research work.

Acknowledgements

S. A. acknowledges the Shaheed Benazir Bhutto University, Shaheed Benazir abad for financial support during the study visit at the Luleå University of Technology Sweden as part of her PhD program. A. V. acknowledges the European Commission under grant agreement GA 654002, the Wallenberg Foundation, the Swedish Foundations, the Kempe Foundation, the LTU Lab fund program and the LTU Seed project for partial funding. The authors are grateful to Prof. I. Lundström for his suggestions and constructive discussions during the preparation of the manuscript. ICN2 and IREC acknowledge funding from Generalitat de Catalunya 2014 SGR 1638 and the Spanish MINECO coordinated projects TNT-FUELS and e-TNT (MAT2014-59961-C2). ICN2 acknowledges support from the Severo Ochoa Programme (MINECO, Grant no. SEV-2013-0295) and is funded by the CERCA Programme/Generalitat de Catalunya. Part of the present work has been performed in the framework of UniversitatAutònoma de Barcelona Materials Science PhD program.

References

1 A. Pizzariello, M. Stredanský, S. Stredanská and S. Miertuš, *Talanta*, 2001, **54**, 763–772.
2 P. S. Francis, S. W. Lewis and K. F. Lim, *TrAC, Trends Anal. Chem.*, 2002, **21**, 389–400.
3 V. Bisht, W. Takashima and K. Kaneto, *Biomaterials*, 2005, **26**, 3683–3690.
4 V. Singh, P. C. Mondal, M. Chhatwal, Y. L. Jeyachandran and M. Zharnikov, *RSC Adv.*, 2014, **4**, 23168–23176.
5 R. A. Soomro, A. Nafady, Z. H. Ibupoto, S. T. H. Sherazi, M. Willander and M. I. Abro, *Mater. Sci. Semicond. Process.*, 2015, **34**, 373–381.
6 Q.-u.-A. Baloach, A. Tahira, A. Mallah, M. Abro, S. Uddin, M. Willander and Z. Ibupoto, *Sensors*, 2016, **16**, 1878.
7 B. K. Boggs, R. L. King and G. G. Botte, *Chem. Commun.*, 2009, 4859–4861.
8 M. Koebel and M. Elsener, *J. Chromatogr. A*, 1995, **689**, 164–169.
9 C. J. Patton and S. Crouch, *Anal. Chem.*, 1977, **49**, 464–469.
10 L. S. Simeral, *Appl. Spectrosc.*, 1997, **51**, 1585–1587.
11 D. Lefier, *Analytical methods for the determination of the urea content in milk*, Federation Internationale de Laiterie-International Dairy Federation, Poligny, France, 1996.
12 R. T. Marshall, *Standard methods for the examination of dairy products*, 16th edn,1992.
13 A. Ramsing, J. Růžička and E. Hansen, *Anal. Chim. Acta*, 1980, **114**, 165–181.
14 F. Roch-Ramel, *Anal. Biochem.*, 1967, **21**, 372–381.
15 X. Hu, N. Takenaka, M. Kitano, H. Bandow, Y. Maeda and M. Hattori, *Analyst*, 1994, **119**, 1829–1833.
16 O. Boubriak, A. Soldatkin, N. Starodub, A. Sandrovsky and A. El'skaya, *Sens. Actuators, B*, 1995, **27**, 429–431.
17 I. Wałcerz, R. Koncki, E. Leszczyńska and S. Głąb, *Anal. Chim. Acta*, 1995, **315**, 289–296.
18 J. Bobacka, A. Ivaska and A. Lewenstam, *Electroanalysis*, 2003, **15**, 366–374.
19 A. P. Soldatkin, J. Montoriol, W. Sant, C. Martelet and N. Jaffrezic-Renault, *Mater. Sci. Eng. C*, 2002, **21**, 75–79.
20 A. Kaushik, P. R. Solanki, A. A. Ansari, G. Sumana, S. Ahmad and B. D. Malhotra, *Sens. Actuators, B*, 2009, **138**, 572–580.
21 M. Zhybak, V. Beni, M. Y. Vagin, E. Dempsey, A. P. F. Turner and Y. Korpan, *Biosens. Bioelectron.*, 2016, **77**, 505–511.
22 C. N. Rao, *J. Mater. Chem.*, 1999, **9**, 1–14.
23 S. K. Meher and G. R. Rao, *J. Phys. Chem. C*, 2011, **115**, 25543–25556.
24 S. Chen, W. Xing, J. Duan, X. Hu and S. Z. Qiao, *J. Mater. Chem. A*, 2013, **1**, 2941–2954.
25 C. Yuan, H. B. Wu, Y. Xie and X. W. D. Lou, *Angew. Chem., Int. Ed.*, 2014, **53**, 1488–1504.
26 G. R. Patzke, Y. Zhou, R. Kontic and F. Conrad, *Angew. Chem., Int. Ed.*, 2011, **50**, 826–859.
27 K. A. Dick, *Prog. Cryst. Growth Charact. Mater.*, 2008, **54**, 138–173.
28 U. Yogeswaran and S.-M. Chen, *Sensors*, 2008, **8**, 290.
29 M. Vidotti, M. Silva, R. Salvador, S. C. de Torresi and L. Dall'Antonia, *Electrochim. Acta*, 2008, **53**, 4030–4034.
30 M. Arain, A. Nafady, Z. H. Ibupoto, S. T. H. Sherazi, T. Shaikh, H. Khan, A. Alsalme, A. Niaz and M. Willander, *RSC Adv.*, 2016, **6**, 39001–39006.
31 L. Qian, L. Gu, L. Yang, H. Yuan and D. Xiao, *Nanoscale*, 2013, **5**, 7388–7396.
32 M. A. Prathap, B. Satpati and R. Srivastava, *Electrochim. Acta*, 2014, **130**, 368–380.
33 R. Ding, L. Qi, M. Jia and H. Wang, *Electrochim. Acta*, 2013, **113**, 290–301.
34 Z. H. Ibupoto, A. Nafady, R. A. Soomro, S. T. H. Sherazi, M. I. Abro and M. Willander, *RSC Adv.*, 2015, **5**, 18773–18781.
35 M. Hussain, Z. Ibupoto, M. Abbasi, X. Liu, O. Nur and M. Willander, *Sensors*, 2014, **14**, 5415.
36 X. Liu, J. Huang, X. Wei, C. Yuan, T. Liu, D. Cao, J. Yin and G. Wang, *J. Power Sources*, 2013, **240**, 338–343.
37 D. A. Daramola, D. Singh and G. G. Botte, *J. Phys. Chem. A*, 2010, **114**, 11513–11521.

38 N. Senthilkumar, G. Gnana Kumar and A. Manthiram, *Adv. Energy Mater.*, 2018, **8**, 1702207.
39 A. Shrivastava and V. B. Gupta, *Chron. Young Sci.*, 2011, **2**, 21.
40 C. C. McCrory, S. Jung, J. C. Peters and T. F. Jaramillo, *J. Am. Chem. Soc.*, 2013, **135**, 16977–16987.
41 Y. Zang, S. Niu, Y. Wu, X. Zheng, J. Cai, J. Ye, Y. Xie, Y. Liu, J. Zhou and J. Zhu, *Nat. Commun.*, 2019, **10**, 1217.
42 I. Katakis and E. Domínguez, *TrAC, Trends Anal. Chem.*, 1995, **14**, 310–319.